Applied Surface Science 422 (2017) 1007–1014

Contents lists available at ScienceDirect

Applied Surface Science

journal homepage: www.elsevier.com/locate/apsusc

Full Length Article

W-containing oxide layers obtained on aluminum and titanium by PEO as catalysts in thiophene oxidation

V.S. Rudnev[a,b,**], I.V. Lukiyanchuk[a], M.S. Vasilyeva[a,b], V.P. Morozova[a], V.M. Zelikman[c], I.G. Tarkhanova[c,*]

[a] Institute of Chemistry, Far-Eastern Branch, Russian Academy of Sciences, Vladivostok, Russia
[b] Far Eastern Federal University, Vladivostok, Russia
[c] M.V. Lomonosov Moscow State University, Moscow, Russia

ARTICLE INFO

Article history:
Received 21 March 2017
Received in revised form 17 May 2017
Accepted 6 June 2017
Available online 10 June 2017

Keywords:
Plasma electrolytic oxidation
W-containing coatings
Metal-supported catalysts
Thiophene oxidation

ABSTRACT

W-containing oxide layers fabricated on titanium and aluminum alloys by Plasma electrolytic oxidation (PEO) have been tested in the reaction of the peroxide oxidation of thiophene. Samples with two types of coatings have been investigated. Coatings I contained tungsten oxide in the matrix and on the surface of amorphous silica-titania or silica-alumina layers, while coatings II comprised crystalline WO_3 and/or $Al_2(WO_4)_3$. Aluminum-supported catalyst containing a smallest amount of transition metals in the form of tungsten oxides and manganese oxides in low oxidation levels showed high activity and stability.

1. Introduction

The more stringent limitations on the content of sulfur in the petroleum raw materials stimulated in recent years new research dealing with catalytic desulfurization processes. The key trend in the purification of liquid hydrocarbon raw materials is hydrotreatment in which sulfur is removed as hydrogen sulfide, which is then subjected to the Claus process to be converted to elemental sulfur [1–4]. However, the achievable degree of sulfur removal is now insufficient; in addition, this brings about new environmental problems related to the storage of sulfur. Therefore, hydrogen-free processes are being rapidly developed based on adsorption, oxidation, and extraction as well as biodesulfurization [5–15]. Recently, the method of oxidative desulfurization (ODS) with H_2O_2 as an oxidizing agent has become one of the most widely used for the desulfurization of petroleum fractions [16–18]. The homogeneous process is conducted in the presence of organic (acetic or formic) or mineral acids [19]. In case of the heterogeneous reaction, a number of individual and mixed oxides and salts containing transition metals, in particular V, Nb, Mo, W, Cr, Zr, Fe, Zn, Cu, Co, Ni, are used as catalysts [20–24]. In Ref. [20], the effective catalytic oxidative desulfurization of diesel fraction by hydrogen peroxide was conducted in the presence of such compounds as Na_2MoO_4, Na_2WO_4, $NaVO_3$, WO_3, WO_3&903;H_2O and $H_3PMo_6W_6O_{40}$, at that the W-containing compounds showed the most activity. The best results were achieved by using the tungsten acid (WO_3&903;H_2O), as well as the mixed heteropoly tungstate/molybdate complexes. The application of active compounds grafted on mineral carriers simplified the process of separating the catalyst and reduced the consuming of transition metals. Silicates [25,26], aluminum oxide, aluminosilicates [10,19], and titanium oxide [27,28] are usually used as carriers.

In some cases it is convenient to use catalysts fixed on a surface of metal substrate – such systems are characterized by high thermal conductivity and mechanical strength, and they can be variously shaped [29–31]. For deposition of the catalytically active substances on a metal substrate, a sublayer or a secondary carrier is required, which improves adhesion to the substrate and increases the specific surface area of the catalyst, as compared with that of metal, and dispersion of the catalytically active components. Such oxide sublayer can be formed by Plasma electrolytic oxidation (**PEO**) technique. The PEO method consists in electrochemical formation of oxide layers on valve metals under spark and microarc electric discharges [32]. This method also has other names: anodic spark deposition, microarc oxidation, anodizing

* Corresponding author at: M.V. Lomonosov Moscow State University, Moscow, Russia.
** Corresponding author at: Institute of Chemistry, Far-Eastern Branch, Russian Academy of Sciences, Vladivostok, Russia.
E-mail address: rudnevvs@ich.dvo.ru (V.S. Rudnev).

http://dx.doi.org/10.1016/j.apsusc.2017.06.071
0169-4332/

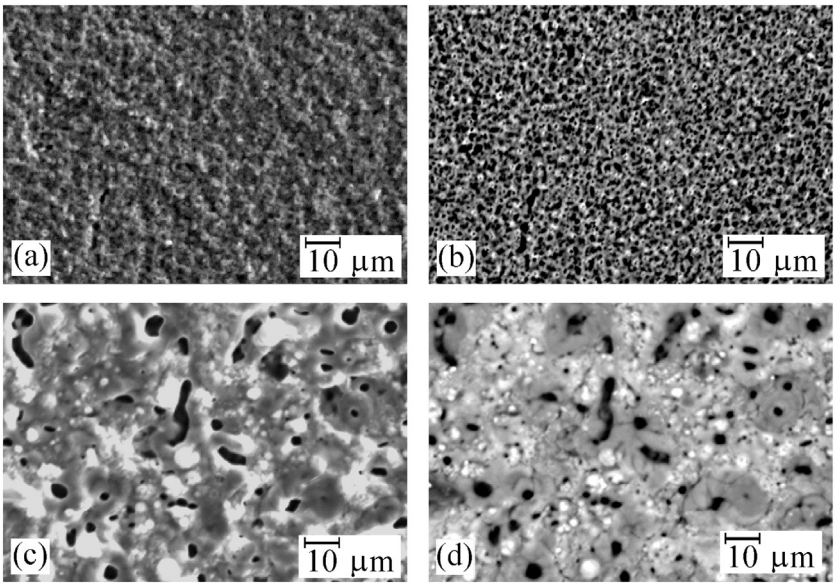

Fig. 1. SEM images of the surfaces of composites I-3 (a, b) and I-5 (c, d) at different contrast: topographic (a, c), compositional (b, d).

at high anodic potentials, anodic spark electrolysis [32]. Several studies have shown that PEO is a promising alternative for fabricating both secondary carriers [33–36], and catalytically active oxide layers [37,38] on metal substrates. This method has been used for obtaining catalysts, which are active in different processes, including CO oxidation into CO_2 [33,34,36,37], afterburning of hydrocarbons [33] and diesel soot [35], oxidative dehydrogenization of cyclohexane to cyclohexene [38], dehydration of ethanol to ethylene [39], conversion of phenol [40] and naphthalene [41], and biomass gasification [42].

PEO technique has been applied for modifying oxide coatings' surfaces by tungsten compounds [39], and for the obtaining crystalline tungsten oxides attached to the surface of titanium and aluminum [43–47], and aluminum tungstate on aluminum surface [45,47]. According to the structure and chemical composition, W-containing PEO layers on aluminum and titanium substrates are expected to be suitable candidates as catalysts for ODS process. The oxide sublayers increase the surface area of the samples and the absence of narrow pores allows to proceed ODS in the kinetic regime. In addition, the oxide sublayers can adsorb the ODS products that significantly increases the efficiency of the process [4,10,11]. At the same time, the catalytic activity of W-containing PEO coatings in the oxidative desulfurization has not been investigated. From the technological point of view, it is important that the production of such catalytic systems is a one-stage process, the spent catalyst on a metallic carrier can be easily separated from the reaction mixture and, as a result, it can be reused and, if necessary, restored. The PEO technique can be promising for obtaining rather cheap W-containing catalysts fixed to the metal substrate for ODS process.

As the object of the study, we chose PEO layers formed: (1) on titanium (and aluminum) in the silicate electrolytes with addition of 0.08–0.023 mol/L Na_2WO_4 [39], (2) on aluminum in electrolytes containing 0.1 mol/L W (VI) in the form of Na_2WO_4, $(NH_4)_{10}[H_2W_{12}O_{42}]$·or $Na_2H[PW_{12}O_{40}]$·[43–47]. According to [39,43–47] coating thickness is in the range of 10–20 μm.

As a model substrate, we used thiophene that is most difficult oxidizable compound among sulfur derivatives contained in petroleum raw [48].

Objective of the work is a comparative analysis of the catalytic properties of aluminum and titanium-supported W-containing oxide layers in the model reaction of thiophene oxidation in hydrocarbon medium.

2. Experimental

2.1. Materials and reagents

PEO-coatings were fabricated on flat samples of a size of 22 × 22 mm or 10 × 40 mm made from sheet technical aluminum (Al > 99.3%) of a thickness of 0.3 mm, aluminum alloy Al-Mn (Al + 1.6% Mn) of a thickness of 0.5 mm, and VT1-0 titanium (99.9% Ti) foil of a thickness of 0.1 mm. To standardize pre-coating sample surfaces, they were chemically polished to high luster (surface finish class 8–9) in a mixture of concentrated acids. A mixture of H_3PO_4:H_2SO_4:HNO_3 = 4:2:1 (by volume) at 110–120 °C and a mixture of HF:HNO_3 = 1:3 (by volume) at 70 °C were used for treating aluminum and titanium, respectively. Then the samples were washed with distilled water and dried by air at 70 °C.

Electrolytes for plasma electrolytic oxidation contained sodium tungstate, phosphotungstate, or ammonium paratungstate. To prepare the electrolytes, we used distilled water and reagents such as analytical grade $(NH_4)_{10}[H_2W_{12}O_{42}]\cdot 10H_2O$, reagent-grade $Na_2WO_4\cdot 2H_2O$ and $Na_2H[PW_{12}O_{40}]$ xH_2O, $Na_2SiO_3\cdot 9H_2O$, H_3BO_3, $Na_3PO_4\cdot 12H_2O$, and CH_3COOH. Ammonium paratungstate was dissolved under heating to 70 °C. Electrolyte compositions, the modes of PEO processing, and coating characteristics are shown in Tables 1 and 2.

2.2. PEO coatings fabrication

Oxide layers were formed on anodically polarized aluminum and titanium samples immersed into electrolytes at effective current densities i = 0.03–0.2 A/cm^2 during t = 5–15 min. A PC-controlled commercial TER-4/460N thyristor unit (Russia) was used as a current source. JSC Fleron (Vladivostok, Russia) developed the synchronizer unit and software. The electrochemical cell consisted of a thermal glass of a volume of 1 L and a cathode in the form of a coil pipe: a hollow tube (0.5 cm in diameter) made of the corrosion-resistant steel of the grade 12 Kh18N10T. Cold tap water was passed through the coil pipe for cooling. The solution was stirred using a magnetic stirrer. The solution temperature during the process did

Table 1
Conditions of PEO treatment of aluminum and titanium samples in silicate electrolytes containing 0.008–0.023 mol/L Na_2WO_4, and composition of PEO coatings.

No.	Forming conditions					Coating composition			Conventional designation of the composite
	Substrate	Electrolyte, mol/L	Electric mode						
			i, A/cm^2	t, min	U_k, V	XRD	C, at.%	C, wt.%	
I-1	Ti	0.1 Na_2SiO_3 + 0.023 Na_2WO_4	0.05	10	160	TiO_2 (anatase)	71.43 O 0.40 Na 9.19 Si 17.57 Ti 1.41 W	45.52 O 0.37 Na 10.28 Si 33.51 Ti 10.32 W	$\frac{1.4\ WO_{3\pm}SiO_{2\pm}TiO_2}{Ti}$
I-2	Ti	0.1 Na_2SiO_3 + 0.008 Na_2WO_4	0.05	10	200	TiO_2 (anatase)	72.06 O 8.62 Si 18.6 Ti 0.71 W	47.72 O 10.02 Si 36.86 Ti 5.40 W	$\frac{0.7\ WO_{3\pm}SiO_{2\pm}TiO_2}{Ti}$
I-3	Ti	0.1 Na_2SiO_3 + 0.015 Na_2WO_4	0.1	10	284	TiO_2 (rutile and anatase)	76.60 O 0.67 Na 14.75 Si 6.89 Ti 1.09 W	54.84 O 0.49 Na 19.46 Si 15.68 Ti 9.51 W	$\frac{1.1\ WO_{3\pm}SiO_{2\pm}TiO_2}{Ti}$
I-4	Ti	0.1 Na_2SiO_3 + 0.015 Na_2WO_4	0.1	5	140	TiO_2 (anatase)	73.69 O 0.47 Na 7.94 Si 16.94 Ti 0.96 W	49.12 O 0.45 Na 9.29 Si 33.79 Ti 7.35 W	$\frac{1.0\ WO_{3\pm}SiO_{2\pm}TiO_2}{Ti}$
I-5	Al-Mn alloy	0.1 Na_2SiO_3 + 0.015 Na_2WO_4	0.1	5	336	γ-Al_2O_3	62.74 O 0.55 Na 26.86 Al 9.01 Si 0.14 Mn 0.70 W	47.11 O 0.59 Na 34.02 Al 11.88 Si 0.36 Mn 6.04 W	$\frac{0.7\ WO_{3\pm}SiO_{2\pm}\gamma\text{-}Al_2O_3}{Al}$

Table 2
Conditions of PEO treatment of aluminum and its alloy in electrolytes containing 0.1 mol/L W(IV) and composition of PEO coatings.

No.	Forming conditions					Coating composition			Conventional designation of the composite
	Substrate	Electrolyte, mol/L	Electic mode			XRD	C, at.%	C, wt.%	
			i, A/cm^2	t, min	U_k, V				
II-1	Al	0.1 Na_2WO_4 + 0.0013 Na_3PO_4; pH 11/12.1	0.2	7	193	WO_3	0.08 Al 16.12 W 0.82 Na 82.98 O	0.05 Al 68.72 W 0.44 Na 30.79 O	$\frac{WO_3}{\frac{Al_2O_3}{Al}}$
II-2	Al-Mn	0.0083 $(NH_4)_{10}W_{12}O_{41}$ + 0.4 H_3BO_3; pH 6.1/6.6	0.05	10	216	WO_3	19.21 W 0.08 Na 80.71 O	73.2 W 0.04 Na 26.76 O	$\frac{WO_3}{\frac{Al_2O_3}{Al}}$
II-3	Al-Mn	0.0083 $Na_2H[PW_{12}O_{40}]$ + 0.083 $KMnO_4$; pH 1.8	0.1	10	224	$WO_{2.9}$	0.18 Al 9.32 W 0.34 P 0.76 Mn 0.08 Na 0.06 K 89.26 O	0.15 Al 53.5 W 0.33 P 1.30 Mn 0.06 Na 0.07 K 44.59 O	$\frac{Mn\text{-}WO_{2.9}}{\frac{Al_2O_3}{Al}}$
II-4	Al-Mn	0.4 H_3BO_3 +0.1 Na_2WO_4 + CH_3COOH; pH 4.0/4.1	0.03	10	204	$Al_2(WO_4)_3$ + $Na_{0.28}WO_3$	9.05 Al 12.27 W 78.68 O	6.5 Al 60.0 W 33.5 O	$\frac{Al_2(WO_4)_3}{\frac{Al_2O_3}{Al}}$
II-5	Al-Mn	0.4 H_3BO_3 +0.1 Na_2WO_4; pH 7.6/7.7	0.03	15	148	WO_3 + amorphous phase	Black sites 5.59 Al 10.2 W 0.05 Mn 0.68 Na 83.43 O Green sites 0.29 Al 20.23 W 79.48 O	 4.45 Al 55.6 W 0.09 Mn 0.46 Na 39.4 O 0.16 Al 74.4 W 25.44 O	$\frac{WO_3}{\frac{Al_2(WO_4)_3}{\frac{Al_2O_3}{Al}}}$

not exceed 35 °C. After PEO treatment, the samples were rinsed by the distilled water and air-dried at room temperature.

2.3. Coatings characterization

X-ray analyzer SUPERPROBE JXA-8100 (JEOL) was used for determining the elemental compositions of the coatings surface parts and obtaining electron microscopic images of the surfaces and element distribution maps. The depth of the analyzed layer was about 2–5 μm. Before the measurements, graphite was sputtered on sample surfaces to create an electrically conductive layer.

In some cases, the data on the samples morphology and element composition were obtained using a Hitachi S5500 high-resolution scanning electron microscope (Japan) equipped with a Thermo Scientific accessory for energy-dispersive analysis (USA). Gold was preliminarily sputtered on the samples to prevent surface charging. The depth of scanning beam penetration was ~1 μm.

The phase coatings compositions were determined previously [39,43–47] from X-ray diffraction (XRD) patterns obtained on X-ray diffractometers DRON-2 (Russia) and Bruker D8 ADVANCE (Germany) in Cu K_α-radiation according to standard procedure. The identification of compounds was carried out in an automatic mode using EVA search program with PDF-2 database.

2.4. Catalytic tests and analysis of the reaction products

A reactor kept in a thermostat was charged with the model mixture (1% solution of thiophene in isooctane (10 mL), 35% H_2O_2 (0.4 mL), and a catalyst (0.1–0.12 g). The mixture was stirred at 60 °C for 1–6 h. Samples were taken at intervals, and the organic phase was analyzed quantitatively by GLC on a Kristall 2000M chromatograph (Chromatec, Russia) equipped with a flame ionization detector and a 3 m long column with SE-30 non-polar phase. Decane was used as the internal reference. The products in the aqueous and organic phases were identified by high resolution mass spectra (HR MS) on a Bruker micrOTOF II instrument using electrospray ionization (ESI) and by 1H NMR on a Bruker Avance-600 instrument (600 MHz for 1H), T = 298 K. To reuse the catalyst, the reaction solution was decanted and the solid sediment was washed by the isooctane. When carrying out additional experiments with catalyst I-5, 50% H_2O_2 was used, and the oxidant was loaded either at once or in batches by 0.2 or 0.4 mL every 1.5–3 hours respectively.

3. Results and discussion

3.1. Coatings composition

Elemental and phase compositions of PEO coatings formed in the electrolytes containing tungtates, as well as isopoly and heteropoly tungtates are shown in Tables 1 and 2. According to these data, the coated samples can be divided into two large groups. The samples with **coatings I** contain about 1 at.% W (VI) in the matrix and on the surface of $SiO_2 + TiO_2$ or $SiO_2 + Al_2O_3$ layers. Outer layers of **coatings II** comprise crystalline tungsten compounds such as WO_3 and $Al_2(WO_4)_3$.

3.1.1. Coatings I

According to XRD, coatings I formed in silicate-tungstate electrolytes comprise crystal oxides of metal substrates; those are titanium dioxide, mainly in form of anatase, for titanium samples and γ-Al_2O_3 for aluminum samples (Table. 1). Despite the relatively high silicon concentration (8–15 at.%) and significant tungsten content (up to 1.4 at.%), crystalline compounds of silicon and tungsten are not found in the coatings compositions. The presence of SiO_2 and WO_3, apparently in an amorphous state, was concluded in [39]

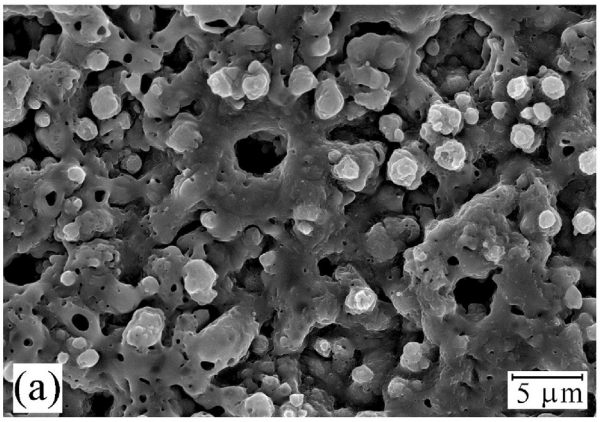

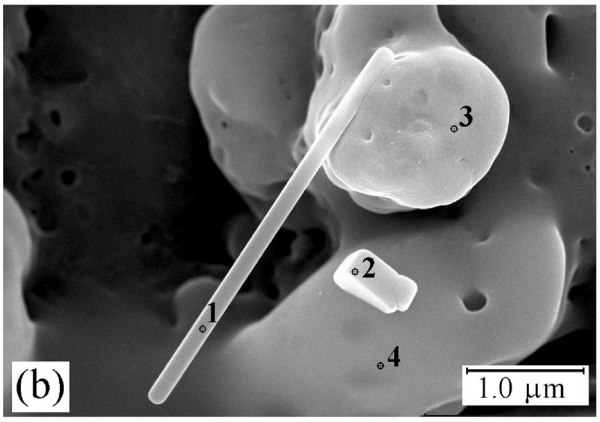

Element	C, at. %			
	1	2	3	4
C	17.77	22.47	13.18	23.45
O	48.54	48.18	66.85	53.90
Na	3.07	8.04	1.00	1.05
Si	19.33	16.58	15.41	18.81
Ti	9.46	3.17	2.06	2.31
W	1.83	1.57	1.51	0.48

Fig. 2. High-resolution SEM images of the surfaces of composites I-3 (a, b) and elemental compositions (at.%) of the sites 1-4.

based on the data of X-ray photoelectron spectroscopy and infrared spectroscopy of samples with similar coatings. Therefore, the composites I hereinafter will be designated as $WO_3 + SiO_2 + TiO_2$/Ti and $WO_3 + SiO_2 + γ\text{-}Al_2O_3$/Al.

The surface of coatings I on titanium (composites $WO_3 + SiO_2 + TiO_2$/Ti) is melted, microporous, and a predominant pore size pore is 1–2 μm (Fig. 1a, b). Under the same conditions, the coating formed on aluminum have larger fragments of the surface relief (Fig. 1c, d), Along with pores of a size of ~1 μm, there are pores of a size of 3–6 μm, some of them merge with each other. Rollers ("hills" or elevations) surround the pores; fused spherical formations of 1–10 μm in diameter are on their surfaces.

High-resolution SEM images of $WO_3 + SiO_2 + TiO_2$/Ti composites (Fig. 2a, b) show that their surface is very developed. There are both protuberances and dispersed particles of regular shape on the surface of the coatings. Analysis of the composition of these particles shows that tungsten concentration in them is somewhat higher

Table 3
The catalytic properties of composites in the oxidation of thiophene (10 mL of 1% thiophene solution in isooctane and 0.4 mL of 35% H_2O_2, 60 °C).

No.	Maximum thiophene conversion (%)	Weight loss (%) after 3 cycles	R_0[a] ($mmol\ L^{-1}\ min^{-1}\ g^{-1}$)	TOF[b] (h^{-1})
I-1	55	1	7.2	53
I-2	48	0.7	5.4	83
I-3	21	0	2.9	23
I-4	28	2	3.0	32
I-5	34	0	2.4	178
II-1	59	8	0.07	13
II-2	46	8	1.1	3.4
II-3	47	10	2.1	14
II-4	45	5	1.4	11
II-5	51	6	2.0	13

[a] R_0 is the initial rate of thiophene consumption, normalized to the catalyst weight.
[b] TOF turnover frequency was calculated as the ratio of the initial rate of thiophene consumption to the tungsten concentration.

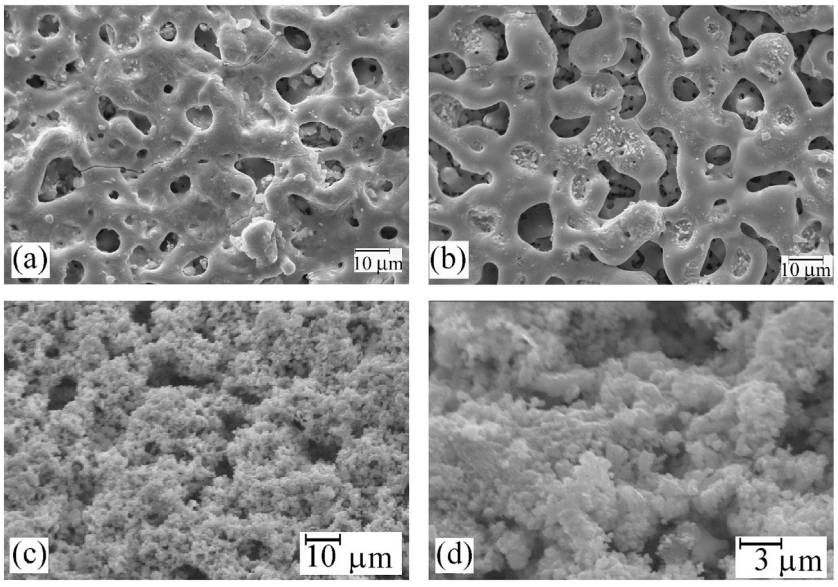

Fig. 3. SEM images (a, b – top view, c, d – the view at the 45° to the surface) of coatings II-4 (a), II-5 (b), II-2 (c, d).

than its average concentration in the coatings. This may indirectly confirm the assumption made in [39] on formation well dispersed clusters of WO_3 on the surface of composite $WO_3 + SiO_2 + TiO_2$/Ti that are embedded into a growing silica layer.

3.1.2. Coatings II

A high content of tungsten (9–20 at.%) is found in the coatings II (Table 2). The coatings have layered structures. Depending on the formation conditions (pH and electrolyte composition, electric charge $Q = I \cdot t$ passed through the cell during the formation of coatings), the outer layer of coating consists of WO_3 (coatings II-1, II-2, II-3, Table 2) or $Al_2(WO_4)_3$ (II-4 coating). It may also contain both phases (coating II-5). The surface of the coatings containing crystalline aluminum tungstate (Fig. 3a) is constructed from drop-threadlike structures, its appearance resembles ornament.

Coatings comprising tungsten oxide in the external layer have a developed surface constructed of spherical fragments of a size of ~1 μm (Fig. 3c, d). Fig. 3b shows the surface of coating, outer layer of which contains both WO_3 (green sites) and $Al_2(WO_4)_3$ (of black color) according to [47]. At the same time, according to the method of preparation, a sublayer of oxide of the metal under treatment will always be located between the coating and the substrate metal. The latter allows us to designate the resulting composites as $WO_3/Al_2O_3/Al$, $Al_2(WO_4)_3/Al_2O_3/Al$, $WO_3/Al_2(WO_4)_3/Al_2O_3/Al$, and Mn-$WO_{2.9}/Al_2O_3/Al$ (for manganese-modified coated sample).

3.2. Catalytic properties of the samples

The catalytic properties of the samples in the model reaction at a molar ratio H_2O_2:thiophene equal to 4 are shown in Table 3. As it can be seen from the Table, the initial oxidation rate (R_0), taken relative to the weight of the corresponding catalyst, is generally higher for samples of the first group. Close to 50% thiophene conversion, it has been able to achieve only for the samples I-1 and I-2. The low values of the maximum conversion of thiophene in cases of the other samples of this group may be because of the deactivation of the catalysts, and the parallel consuming of peroxide due to its catalytic decomposition [49]. On the other hand, the samples of the group II have allowed obtaining a higher substrate conversion under relatively low initial rates. The main drawback of these catalysts is their low stability; the probable reason for deactivation may be due to the poisoning by the sulfur deposition on surface or catalyst destruction [49]. The first reason is unlikely, since the main S-containing product SO_4^{2-} has a low poisoning activity [49]. Furthermore, this deposition should increase the mass of the catalysts, but we have observed the opposite effect. The measurement of the samples' weights after three consecutive cycles of the model reaction showed that virtually all the coating was washed off and tungsten oxide proceeded into the reaction solution. This was also noticeable in the disappearance of the colored sites corresponding to tungsten compounds on the surface of coatings: green sites of WO_3, beige sites of $WO_{2.9}$ and black sites of $Al_2(WO_4)_3$. The

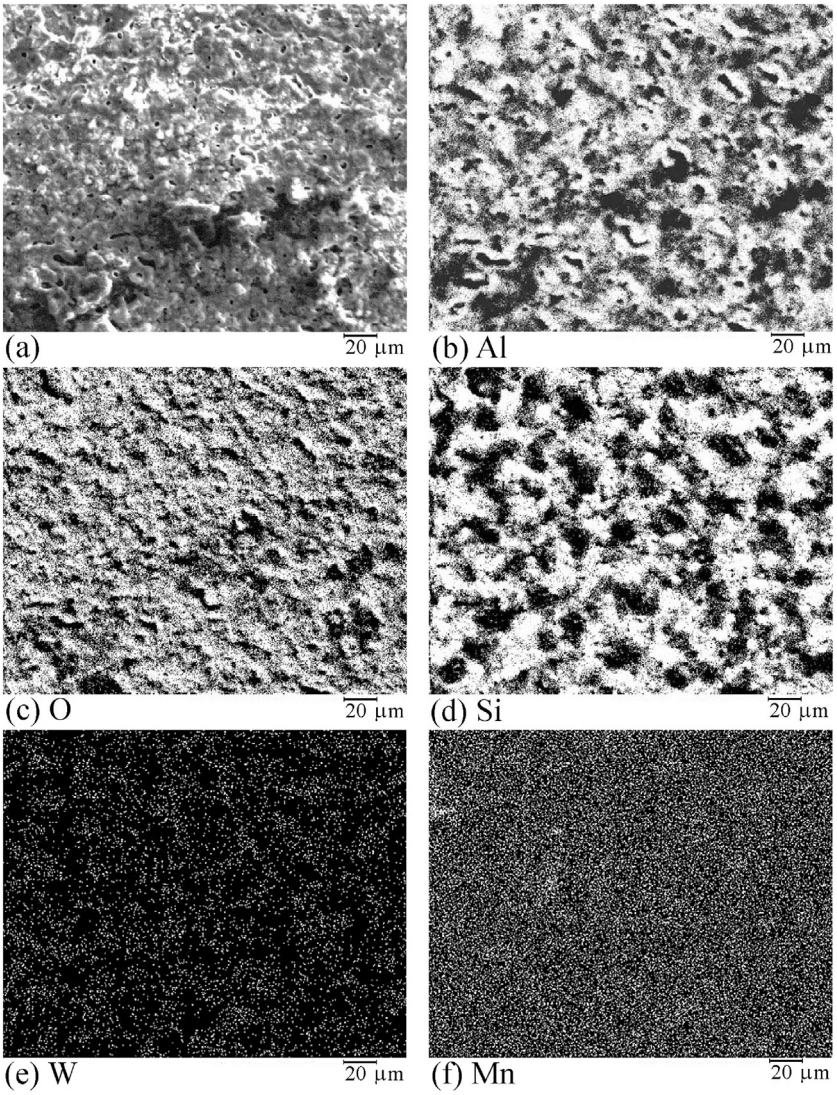

Fig. 4. SEM image of I-5 coating surface (a) and distribution maps of aluminum (b), oxygen (c), silicon (d), tungsten (g), and manganese (e).

loss in weight, although in a lesser degree, was observed for catalysts I-1, I-2 and I-4. The composites $WO_3 + SiO_2 + TiO_2/Ti$ and $WO_3 + SiO_2 + \gamma\text{-}Al_2O_3/Al$, containing WO_3 and SiO_2 in the amorphous state, turned out the most stable.

It should be note that in case of the group I, silicate titanium-oxide layers are apt to display catalytic properties along with the W-containing components. As it was showed in [49–51], the Ti-containing silicate composition carriers (TS-1, Ti/HMS, Ti/MCM-41) were able be used as catalysts in reactions of selective oxidation of sulfur compounds with hydrogen peroxide. Catalyst I-3, however, showed the least activity among the all investigated compositions. Thus, catalyst I-5 has approved oneself as the most perspective for further researches.

After using this catalyst, we analyzed the composition of thiophene oxidation products in the both aqueous and organic phases. According to [19,51–53] reaction proceeds with the formation of sulfate anion, hydrocarbons, such as styrene, carboxylic acids (benzoic, formic) or, in case of the deepest oxidation, carbon dioxide. According to the C^{13} PMR and NMR data, the organic phase contained only thiophene and starting alkanes. The HR MS-technique did not indicated carboxylic acids in the aqueous phase. The addition of $BaCl_2$ to the aqueous phase resulted in a white precipitate of barium sulfate. All these results showed that in the system proceeds deep oxidation of thiophene, accompanied by the destruction of the aromatic structure. Low conversion of thiophene (see Table 3), are obviously the results of lack of hydrogen peroxide. To increase the conversion of thiophene, molar ratio $[H_2O_2]$:[S] not less than 10 is required [52]. To reduce the possible impact of the side reaction of peroxide decomposition and increase the efficiency of its use, we applied the method of fractional loading H_2O. Such technique has been described in the literature on the oxidation of various substrates by hydrogen peroxide [54,55]. Our findings are summarized in Table 4.

Table 4
Total thiophene conversion (%) at different ways of peroxide introducing in the reaction mixture (10 mL of the 1% solution of thiophene in isooctane, 0.1 g of catalyst I-5, 0.8 mL of 50% H_2O_2, 60 °C)

Time, h	The ways of 50% H_2O_2 introducing		
	1 × 0.8 mL	2 × 0.4 mL	4 × 0.2 mL
	Thiophene conversion (%)		
1	27	22	20
3	61	43	49
6	69	77	82

Table 5
The average elemental composition (at.%) of pores, rollers around the pores and surface of I-5 coating according to energy dispersion analysis.

Element	Pores	Rollers	Surface
C	9.6	26.1	26.2
O	35.6	42.2	48.0
Na	0	0.1	0.1
Al	45.4	25.4	15.4
Si	5.3	4.9	8.5
Mn	2.8	0.2	0.2
W	1.3	1.1	1.6
Mn/W	2.2	0.2	0.1

Thus, the fractional loading of peroxide allows significantly increase the thiophene conversion. It should again be noted that the unsubstituted thiophene due to the low electron density on the atom S is the most stable in comparing with the other thiophene derivatives in the hydrocarbon feedstock. Its amount in the total body of S-containing compounds is less than 1%. For example, according to [52] the ability to oxidation decreases in the range BT > 2,3,5–3 MT > 2,5–2MT > 3-MT > 2-MT > thiophene. Therefore, our findings allow us to expect a high ODS capacity of catalyst I-5 in both diesel and gasoline fractions. It was of interest to analyze the possible reasons for the high stability and activity of the catalyst. It differs markedly from the other catalysts in low W content and the presence of commensurate with the latter amount of Mn in the coating.

3.3. Investigation of I-5 catalyst structure

Fig. 4 shows a general view of I-5 coating surface (a) and distribution maps of aluminum (b), oxygen (c), silicon (d), tungsten (g), and manganese (e) obtained by the X-ray analyzer Superprobe JXA-8100 (JEOL). According to SEM images (Fig. 4a), the surface of PEO coating I-5 is non-uniform, it is penetrated with round and oval pores of a size of few microns. The pores are the traces of electrical breakdown channels, under which the coatings are growing. The bulk of the coatings consists of aluminum, silicon and oxygen (Fig. 4b–d). Oxygen is distributed over the surface rather uniformly (Fig. 4c). On the surface, there are regions enriched by aluminum (Fig. 4b) and those with increased content of silicon (Fig. 4d), wherein the second rise over the first. Tungsten and manganese are rather uniformly distributed over the surface, (Fig. 4d, e), and their localizations in the whole coincide, suggesting the formation of mixed oxides or polyoxometallates. As to energy dispersive and microprobe analyzes, coating pores contain increased concentrations of metals from support and electrolyte as well as decreased oxygen concentration (Tables 1 and 5). This allows one to conclude that part of the metals in the coating pores is in the reduced state. A similar phenomenon was observed for different PEO coatings, for example, in refs. [56,57]. Furthermore, in the pores, one can observe an increase in Mn/W atomic ratio. The average value of this ratio is 0.1 in the coating surface, and it is approximately 2.2 in the pores. Thus, the formation of mixed oxides or polyoxometallates of tungsten and manganese of different valences in the pores of the coating may be a possible reason of the I-5 catalyst activity and stability, which are significantly higher than activity and stability of other samples. The catalytic properties of polyoxometallates under oxidizing processes with hydrogen peroxide and a variety of organic substrates are well known from literature [58].

4. Conclusion

For the first time it has been showed that W-containing oxide coatings formed on titanium and aluminum by Plasma electrolytic oxidation technique are active in the catalytic oxidation of thiophene. The coatings on aluminum and titanium including tungsten oxides into silica-titania or silica-alumina matrix are more stable than the layered coatings on aluminum containing crystal tungsten oxides and/or aluminum tungstate in outer layer. Among them, the Al-Mn aluminum alloy-supported coatings containing 0.7 at.% W have higher TOF value and are most stable. The formation of mixed oxides of tungsten and manganese of different valences in the pores of the coating may be a possible reason of their activity. These composites may be promising catalysts for the oxidative desulfurization of heavy fractions of petroleum products.

Acknowledgments

The work was carried out within Russian State Theme No. 265-2014-001 and partially supported by grants of and the Program “Far East” No. 265-20-15-0022.

References

[1] V.C. Srivastava, An evaluation of desulfurization technologies for sulfur removal from liquid fuels, RSC Adv. 2 (3) (2012) 759–783.
[2] H.L. Yin, T.N. Zhou, Y.M. Chai, Y.Q. Liu, C.G. Liu, Application of zeolites in hydrodesulfurization catalysts for deep desulfurization, Prog. Chem. 24 (07) (2012) 1252–1261.
[3] A. Stanislaus, A. Marafi, M.S. Rana, Recent advances in the science and technology of ultra low sulfur diesel (ULSD) production, Catal. Today 153 (1–2) (2010) 1–68.
[4] Z. Ismagilov, S. Yashnik, M. Kerzhentsev, V. Parmon, A. Bourane, F.M. Al-Shahrani, A.A. Hajji, O.R. Koseoglu, Oxidative desulfurization of hydrocarbon fuels, Catal. Rev. Sci.-Eng. 53 (3) (2011) 199–255.
[5] X.M. Wang, H. Wan, M.J. Han, L. Gao, G.F. Guan, Removal of thiophene and its derivatives from model gasoline using polymer–supported metal chlorides ionic liquid moieties, Ind. Eng. Chem. Res. 51 (8) (2012) 3418–3424.
[6] C. Song, X.L. Ma, New design approaches to ultra-clean diesel fuels by deep desulfurization and deep dearomatization, Applied Catalysis B: Environmental 41 (1–2) (2003) 207–238.
[7] A.J. Hernandez-Maldonado, R.T. Yang, Desulfurization of transportation fuels by adsorption, Catal. Rev.-Sci. Eng. 46 (2) (2004) 111–150.
[8] W.S. Zhu, H.M. Li, X. Jiang, Y.S. Yan, J.D. Lu, J.X. Xia, Oxidative desulfurization of fuels catalyzed by peroxotungsten and peroxomolybdenum complexes in ionic liquids, Energy Fuels 21 (5) (2007) 2514–2516.
[9] R. Sundararaman, X.L. Ma, C.S. Song, Oxidative desulfurization of jet and diesel fuels using hydroperoxide generated in situ by catalytic air oxidation, Ind. Eng. Chem. Res. 49 (12) (2010) 5561–5568.
[10] J.L. García-Gutiérrez, G.A. Fuentes, M.E. Hernández-Terán, P. García, F. Murrieta-Guevara, F. Jiménez-Cruz, Ultra-deep oxidative desulfurization of diesel fuel by the $Mo/Al_2O_3–H_2O_2$ system: the effect of system parameters on catalytic activity, Appl. Catal. A-Gen. 334 (1–2) (2008) 366–373.
[11] L. Yang, J. Li, X.D. Yuan, J. Shen, Y.T. Qi, One step non-hydrodesulfurization of fuel oil: Catalyzed oxidation adsorption desulfurization over HPWA–SBA–15, J. Mol. Catal. A-Chem. 262 (1–2) (2007) 114–118.
[12] L. Alonso, A. Arce, M. Francisco, A. Soto, Extraction ability of nitrogen-containing compounds involved in the desulfurization of fuels by using ionic liquids, J. Chem. Eng. Data 55 (9) (2010) 3262–3267.
[13] G.B. Shan, J.M. Xing, H.Y. Zhang, H.Z. Liu, Biodesulfurization of dibenzothiophene by microbial cells coated with magnetite nanoparticles, Appl. Environ. Microbiol. 71 (8) (2005) 4497–4502.
[14] N. Gupta, P.K. Roychoudhury, J.K. Deb, Biotechnology of desulfurization of diesel: prospects and challenges, Appl. Microbiol. Biotechnol. 66 (4) (2005) 356–366.
[15] A.B. Martín, A. Alcón, V.E. Santos, F. Garcia-Ochoa, Production of a biocatalyst of Pseudomonas putida CECT5279 for DBT biodesulfurization: Influence of the operational conditions, Energy Fuels 19 (3) (2005) 775–782.
[16] J.M. Campos-Martin, M.C. Capel-Sanchez, P. Perez-Presas, J.L.G. Fierro, Oxidative processes of desulfurization of liquid fuels, J. Chem. Technol. Biotechnol. 85 (7) (2010) 879–890.
[17] H. Rang, J. Kann, V. Oja, Advances in desulfurization research of liquid fuel, Oil Shale 23 (2) (2006) 164–176.
[18] E. Ito, J.A.R. van Veen, On novel processes for removing sulphur from refinery streams, Catal. Today 116 (4) (2006) 446–460.
[19] L.J. Chen, S.H. Guo, D.S. Zhao, Oxidative desulfurization of simulated gasoline over metal oxide?loaded molecular sieve, Chin. J. Chem. Eng. 15 (4) (2007) 520–523.
[20] E.V. Rakhmanov, A.V. Tarakanova, T. Valieva, A.V. Akopyan, V.V. Litvinova, A.L. Maksimov, A.V. Anisimov, S.V. Vakarin, O.L. Semerikova, Y.P. Zaikov, Oxidative desulfurization of diesel fraction with hydrogen peroxide in the presence of catalysts based on transition metals, Pet. Chem. 54 (1) (2014) 48–50.
[21] L.C. Caero, E. Hernandez, F. Pedraza, F. Murrieta, Oxidative desulfurization of synthetic diesel using supported catalysts –Part I. Study of the operation

conditions with a vanadium oxide based catalyst, Catal. Today 107–08 (2005) 564–569.
[22] Z.E.A. Abdalla, B.S. Li, A. Tufail, Preparation of phosphate promoted Na_2WO_4/Al_2O_3 catalyst and its application for oxidative desulfurization, J. Ind. Eng. Chem. 15 (6) (2009) 780–783.
[23] L.C.A. de Oliveira, N.T. Costa, J.R. Pliego, A.C. Silva, P.P. de Souza, P.S.D. Patricio, Amphiphilic niobium oxyhydroxide as a hybrid catalyst for sulfur removal from fuel in a biphasic system, Appl. Catal. B-Environ. 147 (2014) 43–48.
[24] S. Kumar, V.C. Srivastava, R.P. Badoni, Oxidative desulfurization by chromium promoted sulfated zirconia, Fuel Process. Technol. 93 (1) (2012) 18–25.
[25] V.V.D.N. Prasad, K.E. Jeong, H.J. Chae, Ch.U. Kim, S.Y. Jeong, Oxidative desulfurization of 4,6-dimethyl dibenzothiophene and light cycle oil over supported molybdenum oxide catalysts, Catal. Comm. 9 (10) (2008) 1966–1969.
[26] X.M. Yan, J.H. Lei, D. Liu, Y.C. Wu, L.P. Guo, Oxidative desulfurization of diesel oil using mesoporous phosphotungstic Acid/SiO_2 as catalyst, J. Chinese Chem. 54 (4) (2007) 911–916.
[27] D. Huang, Y.J. Wang, Y.C. Cui, G.S. Luo, Direct synthesis of mesoporous TiO_2 and its catalytic performance in DBT oxidative desulfurization, Micropor. Mesopor. Mater. 116 (1–3) (2008) 378–385.
[28] X.M. Yan, P. Mei, J.H. Lei, Y.Z. Mi, L. Xiong, L. Guo, Synthesis and characterization of mesoporous phosphotungstic acid/TiO_2 nanocomposite as a novel oxidative desulfurization catalyst, J. Mol. Catal. A-Chem. 304 (2009) 52–57.
[29] P. Avila, M. Montes, E.E. Miro, Monolithic reactors for environmental applications –A review on preparation technologies, Chem. Eng. J. 109 (1–3) (2005) 11–36.
[30] G.L. Vaneman, Comparison of metal foil and ceramic monolith automotive catalytic converters, Stud. Surf. Sci. Catal. 71 (1991) 537–545.
[31] A.S. Pratt, J.A. Cairns, Noble metal catalysts on metallic substrates. A new generation of cellular monoliths for emission control, Platinum Metals Rev. 21 (3) (1977) 74–84.
[32] A.L. Yerokhin, X. Nie, A. Leyland, A. Matthews, S.J. Dowey, Plasma electrolysis for surface engineering, Surf. Coat. Technol. 122 (2–3) (1999) 73–93.
[33] S.F. Tikhov, G.V. Chernykh, V.A. Sadykov, A.N. Salanov, G.M. Alikina, S.V. Tsybulya, V.F. Lysov, Honeycomb catalysts for clean-up of diesel exhausts based upon the anodic–spark oxidized aluminium foil, Catal. Today 53 (4) (1999) 639–646.
[34] V.S. Rudnev, L.M. Tyrina, I.V. Lukiyanchuk, T.P. Yarovaya, I.V. Malyshev, A.Yu. Ustinov, Titanium-suported Ce-, Zr-containing oxide coatings modified by platinum or nickel and copper oxides and their catalytic activity in CO oxidation, Surf. Coat. Technol. 206 (2–3) (2011) 417–424.
[35] N.V. Lebukhova, V.S. Rudnev, P.G. Chigrin, I.V. Lukiyanchuk, M.A. Pugachevsky, A. Yu, E.A. Ustinov, T.P. Kirichenko Yarovaya, The nanostructural catalytic composition $CuMoO_4/TiO_2$ + SiO_2/Ti for combustion of diesel soot, Surf. Coat. Technol. 231 (2013) 144–148.
[36] I.V. Lukiyanchuk, E.K. Papynov, V.S. Rudnev, V.A. Avramenko, I.V. Chernykh, L.M. Tyrina, A.Y.U. Ustinov, V.G. Kuryavyi, D.V. Marinin, Oxide layers with Pd–containing nanoparticles on titanium, Appl. Catal. A-Gen. 485 (2014) 222–229.
[37] M.S. Vasil'eva, V.S. Rudnev, L.M. Tyrina, N.B. Kondrikov, A.N. Budina, Composition and catalytic activity of plasma-electrolytic manganese oxide films on titanium, modified with silver compounds, Russ. J. Appl. Chem. 78 (11) (2005) 1859–1863.
[38] F. Patcas, W. Krysmann, Efficient catalysts with controlled porous structure obtained by anodic oxidation under spark-discharge, Appl. Catal. A-Gen. 316 (2007) 240–249.
[39] M.S. Vasilyeva, V.S. Rudnev, A.I. Tulush, P.M. Nedozorov, A.Y.U. Ustinov, WO_x, SiO_2, TiO_2/Ti composites, fabricated by means of plasma electrolytic oxidation, as catalysts of ethanol dehydration into ethylene, Russ. J. Phys. Chem A 89 (6) (2015) 968–973.
[40] D.J. Liu, B.L. Jiang, M. Zhai, Q. Li, Cu (II)-containing micro-arc oxidation ceramic layers on aluminum: formation, composition, and catalytic properties, Mater. Sci. Forum. 695 (2011) 21–24.
[41] M.S. Vasilyeva, V.S. Rudnev, F. Wiedenmann, S. Wybornov, T.P. Yarovaya, X. Jiang, Thermal behavior and catalytic activity in naphthalene destruction of Ce-, Zr- and Mn-containing oxide layers on titanium, Appl. Surf. Sci. 258 (2) (2011) 719–726.
[42] X. Jiang, L. Zhang, S. Wybornov, T. Staedler, D. Hein, F. Wiedenmann, W. Krumn, V. Rudnev, I. Lukiyanchuk, Highly efficient nanoarchitectured Ni5TiO7 catalyst for biomass gasification, ACS Appl. Mater. Interfaces 4 (8) (2012) 4062–4066.
[43] I.V. Lukiyanchuk, V.S. Rudnev, Tungten oxide films on aluminum, and titanium, Inorg. Mater. 43 (3) (2007) 264–267.
[44] V.S. Rudnev, V.P. Morozova, T.P. Yarovaya, T.A. Kaidalova, P.S. Gordienko, W-containing anodic-spark layers on aluminum alloy, Zashchita Metallov 35 (5) (1999) 524–526 (in Russian).
[45] I.V. Lukiyanchuk, V.S. Rudnev, L.M. Tyrina, E.S. Panin, P.S. Gordienko, Anodic-spark layers formed on aluminum alloy in tungstate-borate electrolytes, Rus. J. Appl. Chem. 75 (12) (2002) 1972–1978.
[46] I.V. Lukiyanchuk, V.S. Rudnev, E.S. Panin, T.A. Kaidalova, P.S. Gordienko, Modification with manganese of anodic layers containing tungsten oxides, Russ. J. Appl. Chem. 76 (10) (2003) 1597–1599.
[47] I.V. Lukiyanchuk, V.S. Rudnev, V.G. Kuryavyi, D.L. Boguta, S.B. Bulanova, P.S. Gordienko, Surface morphology, composition and thermal behavior of tungsten-containing anodic spark coatings on aluminium alloy, Thin Solid Films 445 (1) (2004) 54–60.
[48] S. Otsuki, T. Nonaka, N. Takashima, W. Qian, A. Ishihara, T. Imai, T. Kabe, Oxidative desulfurization of light gas oil and vacuum gas oil by oxidation and solvent extraction, Energy Fuels 14 (6) (2000) 1232–1239.
[49] B. Saha, S. Sengupta, Influence of different hydrocarbon components in fuel on the oxidative desulfurisation of thiophene: Deactivation of catalyst, Fuel 150 (2015) 679–686.
[50] P. Ratnasamy, D. Srinivas, H. Knozinger, Active sites and reactive intermediates in titanium silicate molecular sieves, Adv. Catal. 48 (2004) 1–169.
[51] L.Y. Kong, G. Li, X.S. Wang, Mild oxidation of thiophene over TS–1/H_2O_2, Catal. Today 93–5 (2004) 341–345.
[52] B.Y. Zhang, Z.X. Jiang, J. Li, Y.N. Zhang, F. Lin, Y. Liu, C. Li, Catalytic oxidation of thiophene and its derivatives via dual activation for ultra–deep desulfurization of fuels, J. Catal. 287 (2012) 5–12.
[53] L.Y. Kong, G. Li, X.S. Wang, Kinetics and mechanism of liquid–phase oxidation of thiophene over TS–1 using H_2O_2 under mild condition, Catal. Lett. 92 (3–4) (2004) 163–167.
[54] Y.L. Bi, M.J. Zhou, H.Y. Hu, C.P. Wei, W.X. Li, K.J. Zhen, Oxidation of long chain primary alcohols to acids over the quaternary ammonium peroxotungstophosphate catalyst system, React. Kinet. Catal. Lett. 72 (1) (2001) 73–82.
[55] Z.P. Pai, D.I. Kochubey, P.V. Berdnikova, V.V. Kanazhevskiy, I.Y. Prikhod'ko, Y.A. Chesalov, Structure and properties of tungsten peroxopolyoxo complexes –promising catalysts for organics oxidation. I. Structure of peroxocomplexes studied during the stepwise synthesis of tetra(diperoxotungsten)phosphate-tetra-n-butyl ammonium, J. Mol. Catal. A-Chem. 332 (1) (2010) 122–127.
[56] V.S. Rudnev, I.V. Lukiyanchuk, M.S. Vasilyeva, M.A. Medkov, M.V. Adigamova, V.I. Sergienko, Aluminum- and titanium-supported plasma electrolytic multicomponent coatings with magnetic catalytic, biocide or biocompatible properties, Surf. Coat. Technol. 307 (2016) 1219–1235.
[57] A.B. Rogov, O.P. Terleeva, I.V. Mironov, A.I. Slonova, Iron-containing coatings obtained by microplasma method on aluminum with usage of homogeneous electrolytes, Appl. Surf. Sci. 258 (7) (2012) 2761–2765.
[58] R. Neumann, D. Juwiler, Tetrahedron. 52 (26) (1996) 8781–8788.